


Thermodynamic model for polymorphic dislocation core spreading within hexagonal close packed metals

D. C. Chrzan^{ⓧ,*}, Max Poschmann[ⓧ], Ian S. Winter,[†] and Mark Asta

Department of Materials Science and Engineering, University of California, Berkeley, California 94720, USA

 (Received 14 January 2020; revised 17 September 2021; accepted 27 October 2021; published 7 January 2022)

An exactly solvable thermodynamic model for the core structure of $\langle a \rangle$ -type screw dislocations in α -Ti is introduced and used to explore the role in which polymorphic core spreading contributes to the free energy of the dislocation. Each segment of the dislocation core is assumed to be in one of three possible configurations, and the free energy differences per segment between dislocation core spreadings are taken as parameters. It is shown that thermal fluctuations between the core spreadings should be common, even at room temperature, and that these fluctuations can contribute significantly to the free energy. It is also shown that under some circumstances, the core structures can display morphological switching wherein the stable core spreading changes morphology with a change in temperature. The implications for dislocation dynamics and for modeling finite temperature dislocation core properties using molecular dynamics simulations are considered.

DOI: [10.1103/PhysRevMaterials.6.013604](https://doi.org/10.1103/PhysRevMaterials.6.013604)

I. INTRODUCTION

The elastic forces driving dislocation motion are generally understood. The motion of the dislocation results in a reduction of elastic energy, and a straightforward derivation (within linear elasticity) leads to the Peach-Koehler equation for the force on a dislocation [1]. From this perspective, then, the driving force for the motion of the dislocations is similar amongst all materials. What differs from material to material, however, is the response of the dislocations to the forces placed upon them. These responses are, in turn, strongly influenced by the core structures of the dislocations.

The structure and importance of dislocation core structures were first considered by Peierls [2] and Nabarro [3]. As of now, studies of dislocation cores have become more widespread and have been applied to many materials including diamond cubic semiconductors [4–9], body-centered-cubic (BCC) metals [10–15], face-centered-cubic (FCC) metals [16], and hexagonal-close-packed (HCP) [17–20] metals. Many of these calculations have focused on predicting the proper core structure at zero temperature, although some work in diamond cubic semiconductors considered thermal effects [7,8,21] and some explored the thermal properties of dislocation cores in metals [22–24].

Of special interest here are the $\langle a \rangle$ -type screw dislocation cores in the HCP metals Ti and Zr. Farenc *et al.* reported that dislocations within Ti will move by jumps, between locking positions [25], a process that is now termed “jerky” glide. Recently, Clouet *et al.* studied the dislocation cores in Zr and Ti [20]. Using density functional theory (DFT) based total energy methods they predict that, at zero temperature, the $\langle a \rangle$ -type screw dislocation cores in Zr are spread

on the prism plane and that the same cores in α -Ti are spread on the pyramidal planes. The impact on the dynamics was predicted to be profound—dislocations in Zr should glide smoothly, and those in α -Ti should display “jerky” glide, wherein the dislocation moves in short bursts. Clouet *et al.* confirmed these predictions using *in situ* electron microscopy experiments conducted at $T = 150$ K, with T the temperature.

Interestingly, the predicted internal energy difference between the competing core spreadings is approximately $21 \text{ meV}/b$, with b the magnitude of the Burgers vector [20,26,27]. This small energy difference appears to be of the order of the thermal energy per atom in the core, and this suggests that thermal effects may be influencing the dynamics of the dislocations. The purpose of this study is to assess how the energy difference per unit length between competing core structures influences the global structure, and hence dynamics, of the dislocations. In particular, there is a configurational degree of freedom, the local morphology of the dislocation core spreading, that should contribute to the free energy of the dislocations. Accordingly, recent molecular dynamics (MD) simulations focused on the effects of temperature on the morphology of dislocation core spreading in HCP metals [28]. These simulations revealed that the dislocation core spreading is, indeed, influenced by temperature. Evidently, there is a continuous spectrum of core spreading morphologies accessible to the dislocations at finite temperature, and this available disorder affects the dislocation dynamics. One interesting observation from the molecular dynamics simulations is that combinations of non-Schmid stresses and thermal fluctuations may lead to transitions in the predominant core spreading morphology yielding a dislocation core switching transition. Based on these MD simulations and the work of Clouet *et al.*, a transition from prism spreading to pyramidal spreading could have strong implications for the dislocation dynamics. For example, a transition from prism to pyramidal spread core would

*dchrzan@berkeley.edu

†ian.winter@berkeley.edu

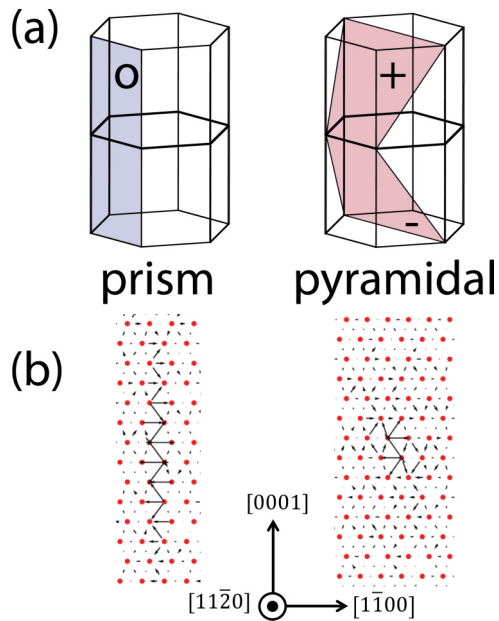


FIG. 1. (a) Three of the planes on which dislocation cores in the HCP metals such as Ti and Zr might be spread. The black wireframe structure represents the unit cell for the crystal. The prism and pyramidal planes are highlighted by color. The prism plane is also indicated by the label “o”, whereas the two pyramidal planes are indicated by a “+” and a “-”. (b) Examples of computed dislocation core structures in Ti that are spread on the prism plane (left) and the pyramidal plane labeled “-” (right). The core structures (as computed using MEAM potentials [30] for the prism spread core, and with an applied non-Schmid stress to stabilize the pyramidal core, as described in Ref. [31]) are depicted using Vitek’s vector map [13,14]. The length of the vector connecting two columns of atoms indicates the relative displacement of the two columns of atoms normal to the page.

lead to locking of the dislocation, and, perhaps, enhanced cross-slip probability.

The phenomenology observed in the molecular dynamics simulations raises a number of interesting questions. For example, how much does dislocation core spreading polymorphism contribute to the free energy of the cores? Can these contributions alone lead to dislocation core switching? Molecular dynamics simulations necessarily involve relatively small cells. Does this influence the observations? If so, what are the effects of finite size?

To explore these and other questions, an exactly solvable thermodynamic model for polymorphic dislocation core spreading of the $\langle a \rangle$ -type screw dislocations in HCP metals is introduced. An Ising-like model is developed [7,8,29] that allows for dislocation core spreading on the prism plane, and two pyramidal planes as described in Fig. 1. The model is solved analytically, and analyzed in detail. The model suggests that core morphology configurational contributions to the free energy become comparable to their zero-temperature energy difference at roughly 300 K. The correlation lengths for the core morphologies are computed, and then related to the expected dynamics of the dislocations. The model also shows that a dislocation core switching transition can be driven by configurational entropy alone, but this is not likely

to be the origin of the transition observed in the molecular dynamics simulations. The model enables studies of the effects of finite size, and demonstrates that in certain circumstances, these effects can be quite strong. Finally, methods for connecting the predictions of the simplified model to the results of molecular dynamics simulations are developed.

II. THERMODYNAMIC MODEL

The thermodynamic model assumes that the dislocation is, on average, straight, and that there are no long range interactions between the differing dislocation core structures. The dislocation line length is divided into units of length b , the magnitude of the Burgers vector for the dislocation. It is further assumed that each section of the dislocation can assume one of three configurations: one prism plane and two pyramidal plane spreadings (Fig. 1). A spin variable σ_i is assigned to each site in the model. The spin variables can take on the three values -1 , 0 , and 1 corresponding to finding the dislocation core at site i dissociated on the pyramidal plane labeled $-$ in Fig. 1, the prism plane labeled with an o in Fig. 1 and the pyramidal plane labeled $+$ in Fig. 1, respectively.

It is noted that the the $+$ pyramidal spread core, and the $-$ pyramidal spread core are displaced by the distance of one Peierls valley in the prism plane, or approximately 2.4 \AA . This implies that there are, in practice, small displacements of the dislocation line that may lead to long-ranged elastic interactions. The present work neglects this contribution to the dislocation core properties so as to retain the simplicity of the thermodynamic model.

Based on these spin variables, the number operators defining the number of core segments of each type at each segment i of the dislocation can be defined:

$$\begin{aligned} n_i^+ &= \frac{1}{2}(1 + \sigma_i)\sigma_i \\ n_i^o &= (1 - \sigma_i^2) \\ n_i^- &= -\frac{1}{2}(1 - \sigma_i)\sigma_i \end{aligned} \quad (1)$$

where the superscripts $+$, o , and $-$ refer to the planes as labeled in Fig. 1. Note that the n_i ’s can only take on the values 0 and 1 . Since there can only be one type of core at each site, only one of the n_i ’s can be 1 , the other two must equal 0 .

Using these occupation variables it is a simple matter to construct an expression for the internal energy enabling computation of the free energy of a dislocation core in which different segments are spread on different slip planes. The free energy difference between pyramidal spread core and the prism spread cores per unit length is defined to be $\varepsilon_p \equiv E_{\text{core}}(\text{pyramidal}) - E_{\text{core}}(\text{prism})$, with $E_{\text{core}}(\text{pyramidal})$ ($E_{\text{core}}(\text{prism})$) the free energy per unit length (here taken to be the magnitude of the Burgers vector b) of an infinite dislocation spread on a pyramidal(prism) plane. In addition, it is assumed that there is an energy cost associated with changing core structures along a single dislocation. These transitions are referred to as “flips” for lack of a better word. The energy cost of a pyramidal core segment adjacent to a prism core segment is defined to be κ_{op} and the energy cost of a pyramidal core dissociated on the $+$ plane adjacent to a pyramidal core dissociated on the $-$ plane is defined to be κ_{pp} . Periodic boundary conditions are imposed

on the dislocation, and all energies are measured relative to the energy of a perfect prism spread dislocation core.

With these definitions and conditions, the core energy of a dislocation that is M segments long is given by (with proper accounting for periodic boundary conditions assumed):

$$E_{\text{core}} = \sum_{i=0}^{M-1} \left\{ n_i^+ \left(\varepsilon_p + \frac{\Delta}{2} \right) + n_i^- \left(\varepsilon_p - \frac{\Delta}{2} \right) + \kappa_{pp} (n_i^+ n_{i+1}^- + n_i^- n_{i+1}^+) + \left(\kappa_{op} + \frac{\delta}{2} \right) (n_i^o n_{i+1}^+ + n_i^+ n_{i+1}^o) + \left(\kappa_{op} - \frac{\delta}{2} \right) (n_i^o n_{i+1}^- + n_i^- n_{i+1}^o) \right\}. \quad (2)$$

In this expression, the parameter Δ is used to break the degeneracy of the dislocation spreading configurations on the $+$ and $-$ planes. For an isolated dislocation within an infinite medium, one expects $\Delta = 0$. However, local variations in the stress, such as that caused by other defects, for example, can break the degeneracy leading to a finite value of Δ . A positive(negative) value of Δ favors spreading on the $-$ ($+$) prism plane. Similarly, the parameter δ reflects the fact that the boundary energies between the prism and two types of pyramidal planes may also differ once the degeneracy is lifted. A positive value of δ increases(decreases) the boundary energy

between the prism spread core state and the $+$ ($-$) pyramidal plane spread core.

After a bit of algebra, one finds that the energy of the dislocation core can be written in terms of the spin variables alone:

$$E_{\text{core}} = \sum_{i=0}^{M-1} \left\{ \left(\frac{\Delta}{2} + \delta \right) \sigma_i + H \sigma_i^2 - J \sigma_i \sigma_{i+1} + \kappa \sigma_i^2 \sigma_{i+1}^2 - \frac{\delta}{2} (\sigma_i^2 \sigma_{i+1} + \sigma_i \sigma_{i+1}^2) \right\}, \quad (3)$$

with $H = \varepsilon_p + 2\kappa_{op}$, $J = \kappa_{pp}/2$, and $\kappa = J - 2\kappa_{op}$.

From the expression for the core energy, the influence of the parameters is clear. $(\frac{\Delta}{2} + \delta)$ acts like a magnetic field and, when positive, favors $\sigma_i = -1$. H yields a positive contribution to the energy for both types of pyramidal cores, and hence favors the prism spreading when positive. The term κ favors adjacent pyramidal cores when negative, though the contribution does not require the pyramidal cores to be identical. J , which is always positive (otherwise, the domain boundary energy between the two differing pyramidal cores would be negative, and this would lead to an instability that is likely not physical), also favors adjacent pyramidal spread segments, but now these must be of the same type to reduce the energy of the core.

The partition function Z is then defined in the usual manner:

$$Z = \sum_{\sigma_0=-1}^1 \cdots \sum_{\sigma_{M-1}=-1}^1 \exp \left[-\beta \sum_{i=0}^{M-1} \left\{ \left(\frac{\Delta}{2} + \delta \right) \sigma_i + H \sigma_i^2 - J \sigma_i \sigma_{i+1} + \kappa \sigma_i^2 \sigma_{i+1}^2 - \frac{\delta}{2} (\sigma_i^2 \sigma_{i+1} + \sigma_i \sigma_{i+1}^2) \right\} \right], \quad (4)$$

with, due to periodic boundary conditions, $\sigma_M = \sigma_0$, and $\beta = 1/k_B T$, with k_B defined to be Boltzmann's constant, and T the temperature.

The partition function can be summed analytically through the use of a transfer matrix t that is symmetric and real. Specifically, the transfer matrix for the model with periodic boundary conditions takes the form:

$$t = \begin{pmatrix} e^{\frac{\Delta}{2} - H - \kappa + J} & e^{\frac{1}{2}(\delta + \frac{\Delta}{2}) - \frac{H}{2}} & e^{-H - \kappa - J} \\ e^{\frac{1}{2}(\delta + \frac{\Delta}{2}) - \frac{H}{2}} & 1 & e^{\frac{1}{2}(-\delta - \frac{\Delta}{2}) - \frac{H}{2}} \\ e^{-H - \kappa - J} & e^{\frac{1}{2}(-\delta - \frac{\Delta}{2}) - \frac{H}{2}} & e^{-\frac{\Delta}{2} - H - \kappa + J} \end{pmatrix}, \quad (5)$$

where the factors of β are incorporated into the (now) dimensionless parameters of the model. (That is, H , J , κ , Δ , and δ are all dimensionless according to the transformation $\beta H \rightarrow H$, etc.) The partition function for a finite-sized system is then given by

$$\begin{aligned} Z &= \text{Tr}[t^M] \\ &= \text{Tr}\Lambda^M \\ &= \lambda_1^M + \lambda_2^M + \lambda_3^M, \end{aligned} \quad (6)$$

with λ_i the i th eigenvalue of the transfer matrix, and

$$\Lambda = S^{-1} t S = \begin{pmatrix} \lambda_1 & 0 & 0 \\ 0 & \lambda_2 & 0 \\ 0 & 0 & \lambda_3 \end{pmatrix}, \quad (7)$$

with S the orthogonal matrix defined with the i th column equal to the (properly normalized) i th eigenvector of t .

In the thermodynamic limit, i.e., $M \rightarrow \infty$, only the largest eigenvalue is relevant. Most atomic scale dislocation dynamics simulations, however, employ relatively small values of M . In what follows, all terms are retained, and the properties of dislocations defined by finite M are studied.

The expectation values for the number operators, i.e., $\langle n_i^o \rangle$, $\langle n_i^+ \rangle$, and $\langle n_i^- \rangle$, are computed in the usual way using the spin matrix σ :

$$\sigma = \begin{pmatrix} -1 & 0 & 0 \\ 0 & 0 & 0 \\ 0 & 0 & 1 \end{pmatrix}. \quad (8)$$

For example, the expectation value of σ_i , denoted $\langle \sigma_i \rangle$ is given by:

$$\langle \sigma_i \rangle = \frac{1}{Z} \text{Tr} \sigma t^M. \quad (9)$$

The expectations of the number operators (and correlations functions, discussed below) require the expectation values of the products of the spin variables. These can be computed using similar expressions.

The expectation values do not give direct insight into the domain size associated with the dislocations. In order to explore this, we introduce the correlation functions $g_o(l)$ and

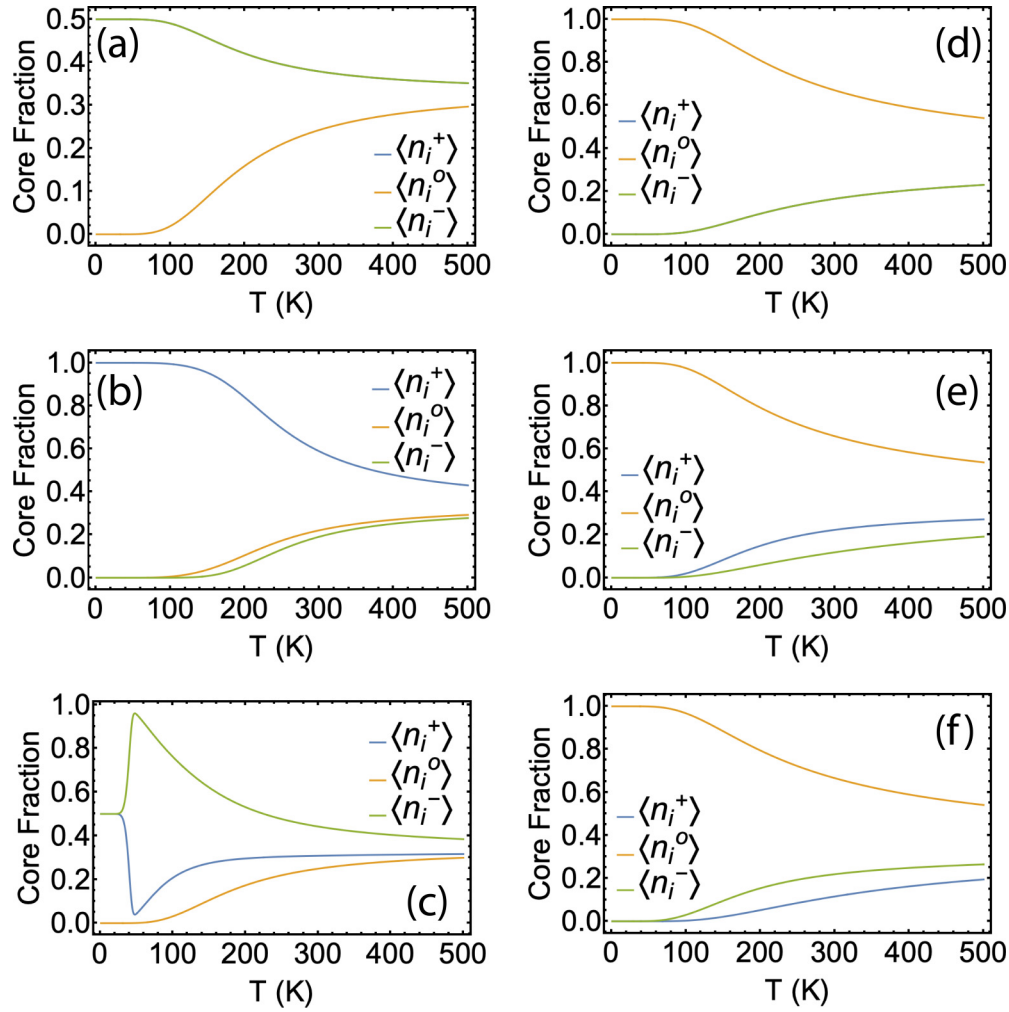


FIG. 2. Expectation values for the core structure number operators plotted as a function of temperature for six different choices of the parameters. For all panels, $\kappa_{op} = 0.01$ eV and $\kappa_{pp} = 0.04$ eV, and $M = 10,000$. Panels (a)–(c) all have $\varepsilon_p = -0.021$ eV. Panels (d)–(f) have $\varepsilon_p = 0.021$ eV. Panels (b) and (e) have $\Delta = -0.01$ eV and $\delta = 0.0$ eV, whereas panels (c) and (f) have $\Delta = 0.0$ eV and $\delta = 0.01$ eV. In panels (a) and (d), $\langle n_i^+ \rangle = \langle n_i^- \rangle$ for all T , and hence both appear as a single line.

$g_+(l)$:

$$g_+(l) = \frac{\langle n_{i+l}^0 n_i^0 \rangle - \langle n_i^0 \rangle^2}{\langle (n_i^0)^2 \rangle - \langle n_i^0 \rangle^2} = \frac{\langle \sigma_{i+l}^2 \sigma_i^2 \rangle - \langle \sigma_i^2 \rangle^2}{\langle \sigma_i^2 \rangle - \langle \sigma_i \rangle^2} \quad (10)$$

and

$$g_+(l) = \frac{\langle n_{i+l}^+ n_i^+ \rangle - \langle n_i^+ \rangle^2}{\langle (n_i^+)^2 \rangle - \langle n_i^+ \rangle^2} = \frac{\langle \sigma_i^2 \sigma_{i+l}^2 + 2\sigma_i^2 \sigma_{i+l} + \sigma_i \sigma_{i+l} \rangle - (\langle \sigma_i^2 \rangle + \langle \sigma_i \rangle)^2}{(2 - \langle \sigma_i \rangle - \langle \sigma_i^2 \rangle)(\langle \sigma_i \rangle + \langle \sigma_i^2 \rangle)}. \quad (11)$$

In the thermodynamic limit ($M \rightarrow \infty$) it is assumed that these correlation functions decay exponentially as they do for the more simple Ising model, and can be described by correlation

lengths ξ_o and ξ_+ :

$$g_o(l) = e^{-l/\xi_o} \\ g_+(l) = e^{-l/\xi_+}. \quad (12)$$

These correlation lengths give a measure of the core structure domain sizes for most cases. For simplicity, the correlation lengths can be determined by solving:

$$g_o(\xi_o) = e^{-1} \\ g_+(\xi_+) = e^{-1}. \quad (13)$$

However, below, it is shown empirically that analytical forms predict exponential decays, but that the longest lived correlations cannot always be identified by solving Eqs. (13).

III. RESULTS AND DISCUSSION

A. Dislocation Structure

The simple model can be used to explore the structure of the dislocation cores, and the influence of temperature. In order to do so, however, one needs reasonable estimates for the

parameters entering the model. The free energy difference per segment between prism and pyramidal spread cores ε_p can be approximated from zero temperature atomic scale total energy calculations. Clouet *et al.* compute the core energy difference between the two structures at $T = 0$ K to be approximately 0.07 eV/Å. Assuming that each of our sites corresponds to a segment of dislocation of length b , then for α -Ti one expects that $\varepsilon_p \approx -0.021$ eV. Of course, the value may change with temperature and/or applied stress [31]. In principle, the “flip” free energies κ_{op} and κ_{pp} can also be computed using atomic scale total energy methods, but these are more difficult to determine accurately. Consequently, these “flip” free energies are treated as parameters, and the changes in core structure as they vary is explored.

For an isolated dislocation in an infinite crystal, one expects that the spreading of the dislocation on either of the pyramidal cores should have the same energy. Therefore, it is typically true that $\Delta = \delta = 0$. However, local stresses can lift the degeneracy, so the dependence of the dislocation core structure on Δ and δ is explored as well.

The potential ground states of the system consist of $\sigma_i = -1$ or $\sigma_i = 1$ for all i , with a corresponding energy of ε_p per site, and $\sigma_i = 0$ for all i , with a ground-state energy of 0 per site. Of course, the model is one dimensional with short-ranged interactions. The implication is that in the thermodynamic limit, the dislocation core is, in principle, disordered, even as $T \rightarrow 0$.

Empirically, one expects that the energy of the “flips” between differing pyramidal plane core spreadings will exceed the energy of a flip between a pyramidal plane spreading and the prism plane core spreading. Therefore, consider the properties of the dislocation cores when $|\varepsilon| = 0.021$ eV, and choose $\kappa_{pp} = 0.04$ eV while choosing $\kappa_{op} = 0.01$ eV. The predictions for these conditions are shown in Fig. 2 for a model containing $M = 10\,000$ sites.

When $\Delta = \delta = 0.0$ eV, the + and – pyramidal cores are degenerate, and have equal population at all temperatures. In the case that $\varepsilon > 0$, these are both the minority species, but each rises to be around 15–20% as the temperature increases from 0 K 300 K.

The +/– symmetry between the pyramidal spread cores can be broken by setting Δ to a nonzero value. In the case that ($\Delta = -0.01$ eV), the + pyramidal spread plane has the lowest on-site energy. For $\varepsilon = -0.021$ eV, the + pyramidal plane is the ground state. As the temperature is increased to 300 K, the core becomes approximately 60% + pyramidal spread, with approximately 20% on each of the prism and – pyramidal plane spreadings, though the prism plane is just slightly more populated. Similar results hold when $\varepsilon = 0.021$ eV, with the roles of the prism and + pyramidal plane spreadings being reversed.

The symmetry can also be broken in the energies of the “flips” as is shown for $\delta = 0.01$ eV. The effects of this parameter are more subtle. Though the energies of the +/– pyramidal spread cores remain degenerate, the excitation spectrum accessible to both structures is different. For a positive δ , the – pyramidal core has a set of excitations accessible to it that are lower in energy than any of those accessible to the + pyramidal core. This has the consequence that the – pyramidal spread core is most common for $T > 50$ K,

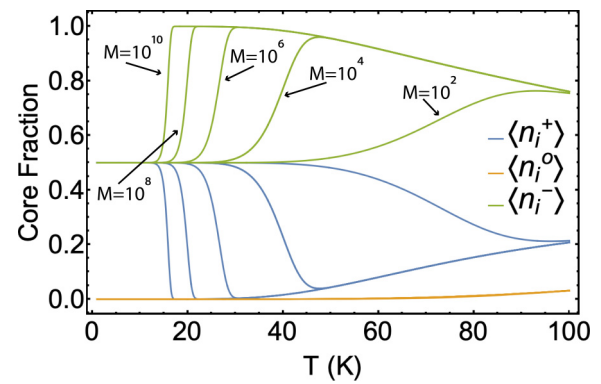


FIG. 3. Expectation values for the core structure number operators plotted as a function of temperature $\kappa_{op} = 0.01$ eV and $\kappa_{pp} = 0.04$ eV, $\varepsilon_p = -0.021$ eV, $\Delta = 0.0$ eV and $\delta = 0.01$ eV for $M = 10^2, 10^4, 10^6, 10^8$, and 10^{10} . The degeneracy as $T \rightarrow 0$ K is a finite size effect. See the text for details.

for $M = 10,000$ and $\varepsilon_o = -0.021$ eV [Fig. 2(c)]. However, the behavior of the model as $T \rightarrow 0$ K is interesting. Figure 2(c) shows that the fraction of pyramidal spread core on the + plane becomes equal to the fraction spread on the – pyramidal plane, with each constituting one-half of the sites.

The origin of this behavior lies in the finite size of the dislocation. As $T \rightarrow 0$ K, the number of flips within the dislocation structure approaches zero. If there are no excitations, then energies of the + and – pyramidal cores are degenerate, and one expects that their fractions would be equal. This will happen only when all the excitations have been “frozen” out of the system. For a finite length dislocation, freezing out all excitations is a possibility. That is, there is a finite temperature at which the probability of finding a single “flip” becomes arbitrarily small. This temperature, however, should depend upon the length of the dislocation. In the thermodynamic limit, in fact, this temperature should go to zero.

Figure 3 displays the behavior for the same set of parameters as in in Fig. 2(c) for different values of M . The degeneracy between the pyramidal cores is broken by the broken symmetry in their flip energies. As discussed above, for any finite-sized system, as shown in the figure, the ground state is truly degenerate, as one can always find a temperature below which there are no flips in the configuration. However, as M increases, the temperature at which the fractions of + and – pyramidal spread cores become equal to one-half decreases. In the thermodynamic limit, $M \rightarrow \infty$, the broken degeneracy between the two pyramidal spread cores persists to $T = 0$ K, so that in the thermodynamic limit, the differing excitation spectrum selects a unique, nondegenerate ground state.

Figure 4 displays the same core fraction results for the case $\kappa_{pp} = \kappa_{op} = 0.01$ eV. The results are very similar to those shown in Fig. 2 with the exception that for $\Delta = 0.00$ eV and $\delta = 0.01$ eV, the $T \rightarrow 0$ K state for $\varepsilon_p = -0.021$ eV appears to include equal concentrations of + and – pyramidal spreadings in the thermodynamic limit.

The effect of the “flip” energies can be explored by considering the effects on the occupations. Figure 5 displays results

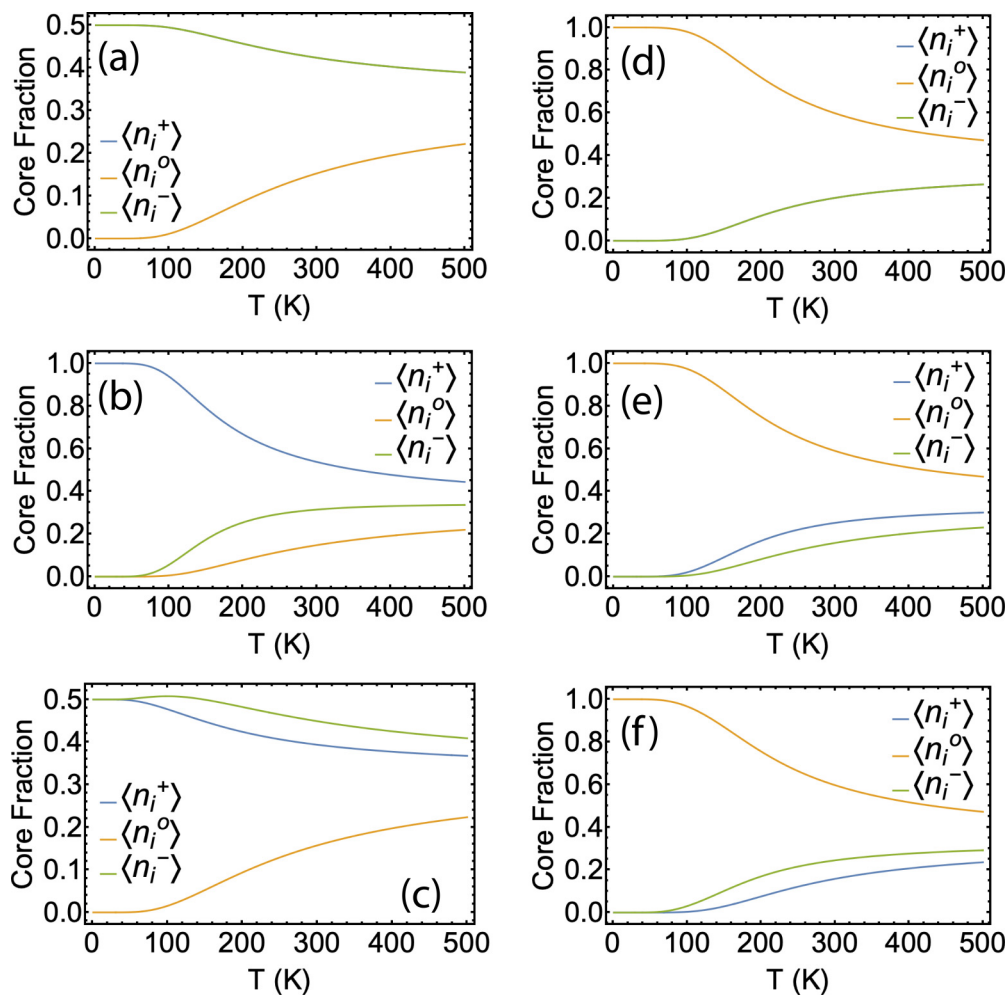


FIG. 4. Expectation values for the core structure number operators plotted as a function of temperature for six different choices of the parameters. For all panels, κ_{op} and κ_{pp} are taken equal to 0.01 eV. Panels (a)–(c) all have $\varepsilon_p = -0.021$ eV. Panels (d)–(f) have $\varepsilon_p = 0.021$ eV. Panels (b) and (e) have $\Delta = -0.01$ eV and $\delta = 0.0$ eV, whereas panels (c) and (f) have $\Delta = 0.0$ eV and $\delta = 0.01$ eV. In panels (a) and (d), $\langle n_i^+ \rangle = \langle n_i^- \rangle$ for all T , and hence both appear as a single line.

similar to those in Fig. 4, but now, as an extreme example (the $+/-$ flip energy exceeds the energy difference between core spreadings), $\kappa_{op} = 0.02$ eV and $\kappa_{pp} = 0.06$ eV. From the figure, it is clear that an increased “flip” energy increases the thermal stability of the structures, but does not much alter the behavior overall, in comparison to Fig. 2.

It is interesting to gauge whether or not polymorphic core spreading can contribute significantly to the free energy of the dislocation core. The model enables the computation of the free energy per site as a function of temperature. Figure 6 displays the free energy per Burgers vector of the dislocation, $F(T)$ computed according to:

$$F(T) = -\frac{k_B T}{M} \ln Z, \quad (14)$$

assuming $\varepsilon_p = -0.021$ eV, and $\Delta = \delta = 0.0$ eV for various choices of κ_{op} and κ_{pp} . For the case $\kappa_{op} = 0.01$ eV and $\kappa_{pp} = 0.04$ eV, at 300 K, the free energy is reduced from the $T = 0$ K state by approximately 0.012 eV/ b . The thermal contribution to the free energy is approximately one-half the $T = 0$ K internal energy difference between the cores computed using DFT. For larger “flip” energies, the reduction in free energy at

300 K is only 0.006 eV, whereas for smaller, but equal “flip” energies, the difference is 0.017 eV. So for the parameters considered here, the thermal contribution to the free energy of polymorphic core spreading is comparable in magnitude to the total internal energy difference between the competing spreading morphologies at $T = 0$ K.

B. Correlations

Of course, the dynamics of the dislocations depend not only on the polymorphic fractions, but also on how those fractions are distributed along the core. The correlation functions introduced above, Eqs. (10) and (11), can provide some insight. Figure 7 displays the correlation lengths computed from Eqs. (13). For the case in which the pyramidal cores are the ground state Fig. 7(a), prism spread core sections remain essentially uncorrelated over the temperature range shown. (ξ_o is less than one over the entire range.) However, the pyramidally spread cores appear to become correlated as the temperature drops. In contrast, if the prism core is the ground state, Fig. 7(b), both types of core segments remain, essentially, uncorrelated over the range of temperatures

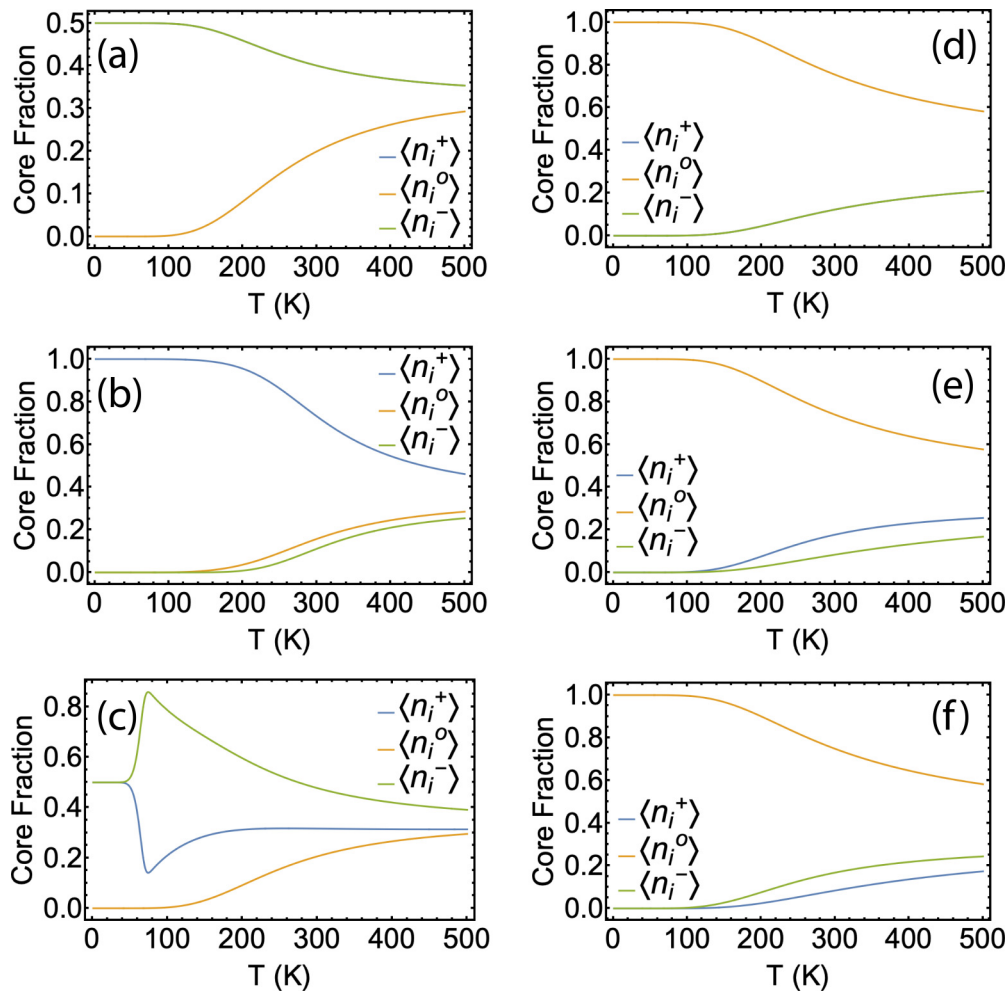


FIG. 5. Expectation values for the core structure number operators plotted as a function of temperature for six different choices of the parameters. For all panels, $\kappa_{op} = 0.02$ eV and $\kappa_{pp} = 0.06$ eV. Panels (a)–(c) all have $\varepsilon_p = -0.021$ eV. Panels (d)–(f) have $\varepsilon_p = 0.021$ eV. Panels (b) and (e) have $\Delta = 0.01$ eV and $\delta = 0.0$ eV, whereas panels (c) and (f) have $\Delta = 0.0$ eV and $\delta = 0.01$ eV. In panel (a), $\langle n_i^+ \rangle = \langle n_i^- \rangle$ for all T , and hence both appear as a single line.

shown. Though not shown in a figure, in the case that the symmetry between core states is broken, then the correlation length again remains quite small for all temperatures.

The fact that the correlation lengths sometimes do not diverge as $T \rightarrow 0$ K can be contrasted with the results from the 1D Ising model in zero field. Whereas the 1D Ising model

in the zero field limit can be thought of as displaying a phase transition precisely at $T = 0$ K, the model for the dislocation core spreading appears to display this behavior only for a very specific set of parameters, for others, there is no increasing correlation length. The origins of this behavior are discussed further below.

To the extent that the correlation lengths reflect the sizes of the domains, these calculations suggest that for the values $\kappa_{op} = 0.1$ eV and $\kappa_{pp} = 0.04$ eV, the domains are quite small. In the case where prism spreading is favorable, the fluctuations to pyramidal spreading must act as a weak pinning point for the dislocation, resulting in a drag that increases with the disorder, i.e., as the temperature, increases. For the case where pyramidal spreading is favored, the pyramidal domains begin to grow below 100 K, and this could lead to jerky glide because the domains of core structure that cannot glide easily on the prism plane are extended in length. Recall that the choice of “flip” energies here is somewhat arbitrary. Increasing them increases the correlation lengths and hence the domain size of cores spread on the pyramidal plane. However, at higher temperatures, the domains again become very small. This does not mean, however, that dislocation motion becomes

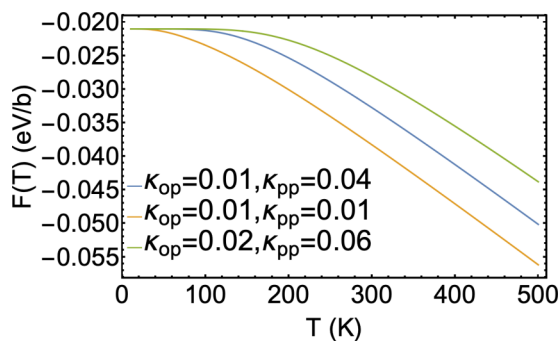


FIG. 6. Free energy curves for $\varepsilon_p = -0.021$ eV, $\Delta = \delta = 0.0$ eV, with different values for “flip” energies, given in eV.

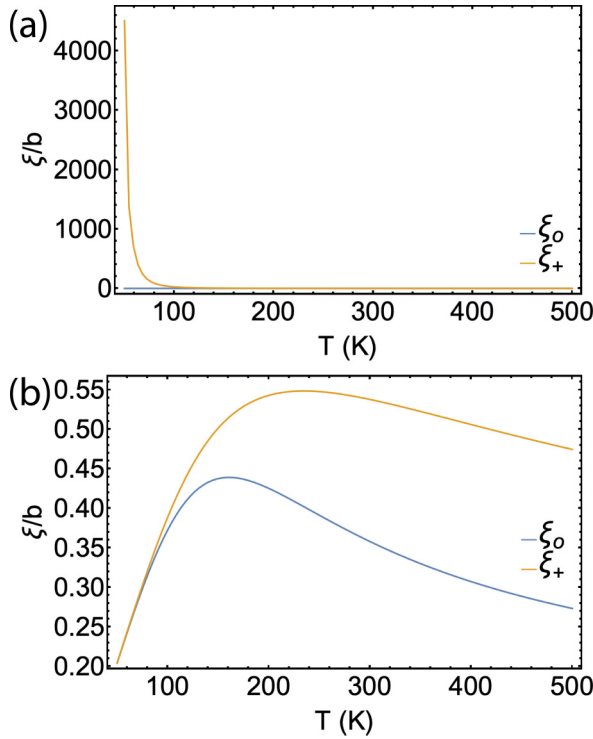


FIG. 7. (a) Correlation lengths for $\varepsilon_p = -0.021$ eV, $\Delta = \delta = 0.0$ eV, $\kappa_{op} = 0.01$ eV, and $\kappa_{pp} = 0.04$ eV. (b) Correlation lengths for $\varepsilon_p = 0.021$ eV, $\Delta = \delta = 0.0$ eV, $\kappa_{op} = 0.01$ eV, and $\kappa_{pp} = 0.04$ eV.

smooth—the dislocation is still predominantly spread on the pyramidal planes even at room temperature.

Interestingly, if the symmetry between pyramidal cores is broken, the correlations appear not to diverge at low temperatures. This behavior is similar to that observed for the case of the prism spreading being the ground state morphology. Examination of the terms in the correlation function $g_+(l)$ reveals the origin of this behavior. In the limit that symmetry between pyramidal spreadings is not broken, all expectations of the spin variables raised to an odd power vanish identically. This implies that the correlation function takes on the following form:

$$g_+(l) \rightarrow g_+^{\text{sym}}(l) = \frac{\langle \sigma_i^2 \sigma_{i+l}^2 + \sigma_i \sigma_{i+l} \rangle - \langle \sigma_i^2 \rangle^2}{(2 - \langle \sigma_i^2 \rangle) \langle \sigma_i^2 \rangle}. \quad (15)$$

Examination of the terms entering the correlation function and their dependence on l , reveals that the l -dependence of $g_+^{\text{sym}}(l)$ is dominated by the correlation $\langle \sigma_i \sigma_{i+l} \rangle$. At low temperature, the fraction of the core that is in the prism spread state drops to near zero, and this forces $\sigma_i^{2n} = 1$, with $n \in \text{Integers}$. Hence the only dependence on l arises from the Ising like term in the problem, and the correlations behave similarly to the 1D Ising model in zero field. However, in the case that the $\langle \sigma_i \rangle$ is nonzero, or if the symmetry between pyramidally spread cores is broken, the correlations behave differently, and the Ising term is only one of many terms contributing to the free energy, which now includes contributions from terms linear in $\langle \sigma_i \rangle$. These terms are similar to those for the 1D Ising model with a finite magnetic field, and no transition at $T = 0$ K is expected.

For the case of $\varepsilon_p > 0$, when the prism core is the ground state, the correlation function, Eq. (10), does not include an Ising-like term, and again, there is no divergence of the correlation length as $T \rightarrow 0$ K.

So, for typical parameters, correlation lengths remain quite small, except for very low temperatures under specific conditions. The implication is that the domain sizes at typical deformation temperatures are quite small. This observation holds implications for dislocation drag and, perhaps, dislocation cross slip rates.

C. Dislocation Core Switching

1. parameter driven core switching

The question of whether or not the model can display a temperature driven switching from, for example, prism spreading to pyramidal spreading, is of some interest. Since the core morphology dictates the dislocation dynamics, such transformations might lead to significant changes in mobility. Atomic scale studies have shown that stresses (both Schmid and non-Schmid) can alter dislocation spreading morphologies, even to the point of altering the ground state structure (at least within empirical potential models) [31]. So the most obvious manner in which the model might display a spreading morphology transition is for the free energy difference per segment (ε_p) between the dislocation cores to change sign, either due to local non-Schmid or Schmid stresses. In additions, the different core spreading morphologies certainly have different phonon spectra, and this will lead to changes in the internal free energy per unit length similar to those computed for diamond cubic semiconductor [8,21]. The model enables study of this type of transition in principle, but in practice the situation is more complicated. Since there is no good model for the free energy difference between core types, and/or the flip free free energies, it is difficult to make a predictions about how the core switching transition will appear. Purely as an example of what might transpire, Figs. 8(a) and 8(b) plot the results expected for a model in which the parameters governing the simulation vary with temperature as shown in Fig. 8(c). The core switching transition temperature was set to be 100 K. Note that the core switching transition is marked by a cusp in the core fraction curves for both the case where pyramidal spread cores are degenerate in energy, and for the case that the degeneracy is broken. Though these results are obtained for $M = 10\,000$, they have converged to the thermodynamic limit.

Dislocation switching transitions may hold implications for experimental measurements as well. Molecular dynamics simulations suggest that these might be observed if the ground-state core spreading morphology is prism spread, as is expected for Zr. This does not appear to be the case for α -Ti, but is, perhaps, not out of the question. In α -Ti, DFT predicts that the ground state morphology is spread on the pyramidal planes [20,26,27]. It is interesting to note that, a typical cell used to compute the energy difference between core structures contains around 200 atoms. Given that the total energy difference between the two configurations in question is 0.042 eV (there are two dislocations within the unit cell), accepting this value as accurate implies an accuracy of the underlying theory for predicting energy differences of

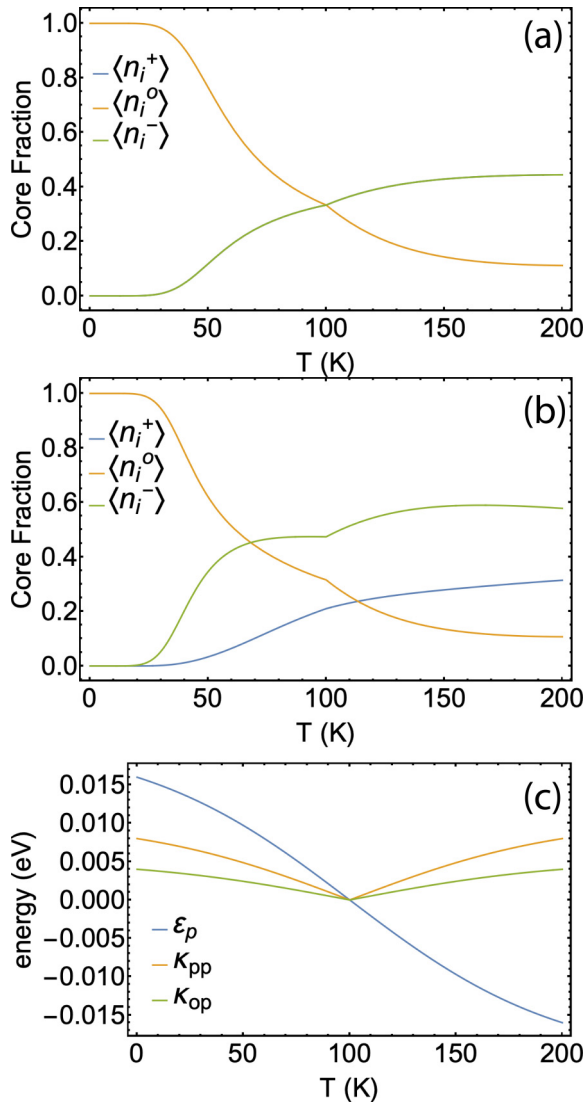


FIG. 8. The predictions of the model for dislocation core fractions when the parameters are allowed to vary in temperature. Panel (a) displays the predictions for the model using the temperature dependent parameters shown in panel (c) when the symmetry is not broken ($\Delta = \delta = 0.0$ eV). Panel (b) displays the predictions for the same set of parameters, but with $\Delta = 0.007$ eV and $\delta = 0.0$ eV. For both sets of results, $M = 10\,000$.

approximately 0.2 meV/atom. This is likely approaching the limits of current DFT functionals, and may also be influenced by the high density of dislocations within the computation. Given these observations, there is still some uncertainty in the predictions of the dislocation core energies, and perhaps, even the ground state spreading morphology.

Another possibility for observing a dislocation core switching transition could be through alloying experiments. In Zr, the morphology of the core is predicted to be spread on the prism plane. The opposite is true of α -Ti. It is possible that by alloying the two elements in different ratios, one might be able to fabricate an alloy in which the dislocations would display the core switching transition. These should be marked by viscous dislocation motion up to the temperatures corresponding

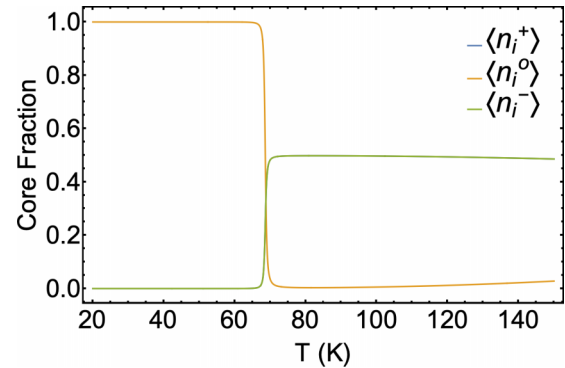


FIG. 9. The dislocation core spreading “composition” as a function of temperature for $\epsilon_p = 0.001$ eV, $\Delta = 0.0$ eV, $\delta = 0.0$ eV, $\kappa_{pp} = 0.01$ eV, and $\kappa_{op} = 0.04$ eV, for a dislocation containing $M = 10^4$ sites. Note that the core switches, rather abruptly, though not with a step function singularity, from being primarily prism spread, to spreading on both pyramidal planes at a temperature near 70 K.

to the core switching transition, wherein thermally activated “jerky” glide would set in.

The analysis above was carried out for one specific *ad hoc* set of parameters, and is meant to demonstrate one possibility regarding the temperature dependence of the parameters. In addition, there is substantial computational evidence that the difference in internal energy between competing core spreadings is also stress state dependent [31]. The same most likely holds for the other parameters of the model. If so, the parameters describing a dislocation within a pileup, for example, may differ from dislocation to dislocation, even if all dislocations are at the same temperature. In fact, it is even possible in principle for two different portions of a single dislocation to be described by differing model parameters. Given these observations, the modeling of dislocation dynamics under realistic conditions of fluctuating stresses and reasonable temperatures poses a significant theoretical challenge.

2. entropy driven switching transition

The model raises another possibility that is interesting to explore, although it is not a likely scenario for the dislocations. Consider the situation in which the prism spread core is just slightly favored ($\epsilon_p > 0.0$ eV), and choose the flip energies so that κ_{op} is significantly larger than κ_{pp} . In these circumstances, as $T \rightarrow 0$ K, the prism spread core will become the dominant core fraction. However, the pyramidal spread cores will have significantly more low-energy excitations available to them. This raises the possibility that as the temperature increases, the core fraction might be dominated by pyramidal spread cores, due to the associated increase in entropy.

To explore this possibility, take $\epsilon_p = 0.001$ eV. Then, take the flip energy between pyramid and prism spread cores to be quite high, $\kappa_{op} = 0.04$ eV, whereas $\kappa_{pp} = 0.01$ eV. For simplicity, choose $\Delta = \delta = 0.0$ eV, for a dislocation with $M = 10\,000$. Figure 9 shows that the dislocation core spreading changes rather abruptly from being spread in the prism plane, to spreading on the pyramidal planes at a temperature just slightly below 70 K. We refer to this phenomenon as an entropy driven switching transition.

The nature of the entropy driven dislocation core switching can be explored by examining the behavior of the correlation functions near the transition temperature. Figure 10(a) shows the correlation lengths computed by using Eqs. (13). Clearly, the correlations in the spins are increasing near the switching temperature. These correlations have not diverged, so there does not appear to be a continuous phase transition in the model. Moreover, the model does not display any discontinuity, so strictly speaking, there is no phase transition. (However, the dislocation core switching transition can be made nearly arbitrarily sharp by increasing κ_{op} .) Figure 10(b) plots the correlation function $g_o(l)$ on a log/normal scale. The lines are relatively straight, suggesting that the correlations in n_i^o remain simple exponential decays. However, Fig. 10(c) that plots $g_+(l)$ on a log/normal scale displays an interesting behavior. For these temperatures, the correlations display a more complicated behavior. They decay initially with a short correlation length, and then display longer range correlations characterized by a longer correlation length. This suggests that using Eqs. (13) is not appropriate for $g_+(l)$. Instead, one should consider the slowly decaying tail of the correlation function, and use this exponential cutoff as a measure of the correlation length. The correlation length so computed is shown in Fig. 10(d) that shows a correlation length approaching $350b$ for $g_+(l)$, and, in fact, the correlation lengths for n^o and n^+ are equal.

The switching behavior can persist, even in the case of broken symmetry between the pyramidal spread cores. Figure 11 displays the composition of the dislocation core, and the correlation times for the case $\varepsilon_p = 0.001$ eV, $\Delta = -0.0005$ eV, $\delta = 0.0$ eV, $\kappa_{pp} = 0.01$ eV, and $\kappa_{op} = 0.04$ eV, for a dislocation containing $M = 10^4$ sites. The core structure still displays a switching transition, and that the correlations still peak near the transition. [The correlations lengths for $g_+(l)$ are computed from the long time decay.]

D. Finite Size Effects

The effects of finite size become interesting when one considers atomic scale calculations of dislocation core structures at temperature. Atomic scale calculations will necessarily be limited to relatively small values of M because of size limitations on the unit cells that can be employed. For example, if one employs the unit cells containing dislocation dipoles, the cells have to be quite large in the direction perpendicular to the line direction of the dislocation. If these cells must also be made $1000b$ thick, their size can slow computation times dramatically. For this reason, it is interesting to understand the effects of finite size on the predictions of the model.

As the discussion above makes clear, there are conditions under which the correlation lengths within the model can extend for relatively large distances of $300b$ or more. It stands to reason that if such a system is studied with a system size smaller than $300b$, that the effects of finite size will alter the results. To explore this size dependence, consider the predictions for the same parameters as Figs. 9 and 10 except now, let the values of M vary from 32 to 1024. Figure 12 plots the same core fractions as in Fig. 9 for these values of M . Clearly, for system sizes below the correlation length (computed in the thermodynamic limit), the size has a significant effect on

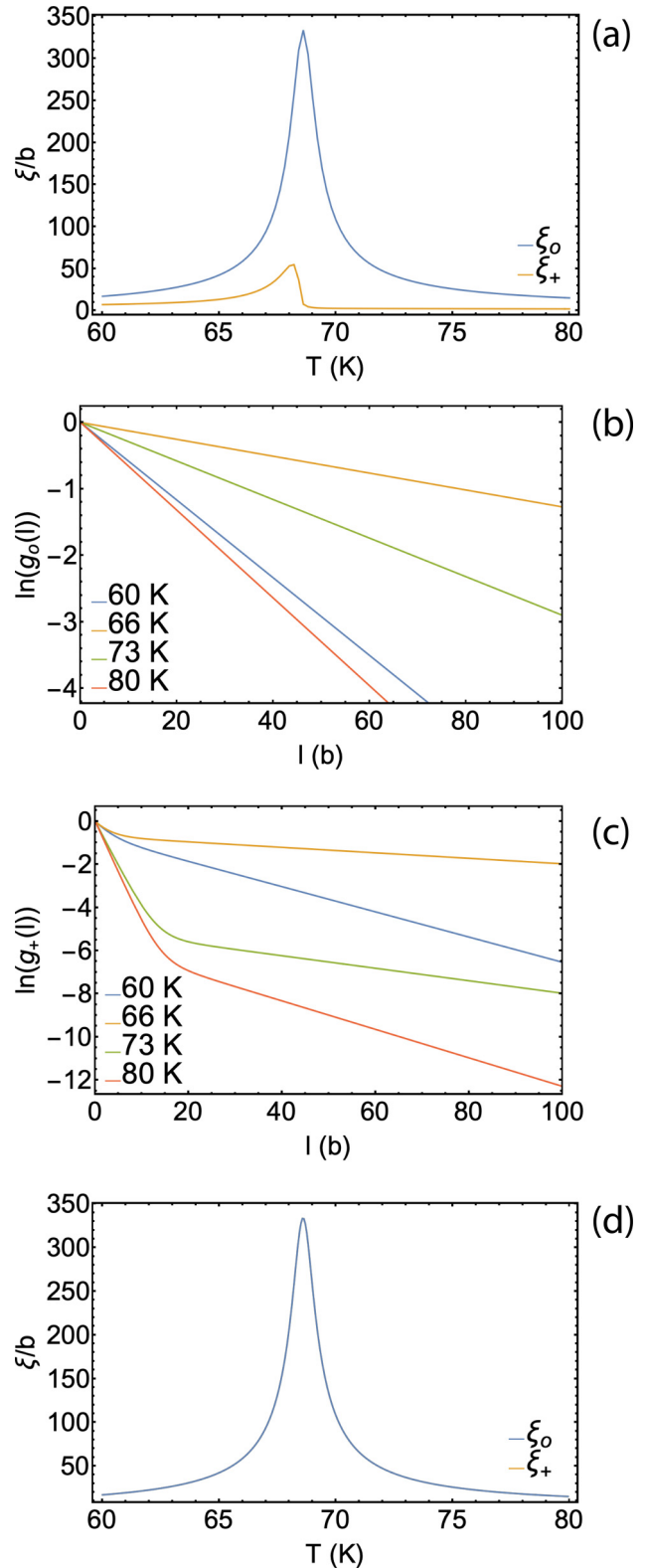


FIG. 10. (a) The correlation lengths computed using Eqs. (12) for a range of temperatures near the switching temperature for $\varepsilon_p = 0.001$ eV, $\Delta = 0.0$ eV, $\delta = 0.0$ eV, $\kappa_{pp} = 0.01$ eV, and $\kappa_{op} = 0.04$ eV, for a dislocation containing $M = 10^4$ sites. (b) Correlation function $g_o(l)$ plotted on a log/normal scale. (c) Correlation function $g_+(l)$ plotted on a log/normal scale. (d) Correlation length for $g_+(l)$ measured from the long time correlations and compared with correlation length computed from n^o . The two curves coincide.

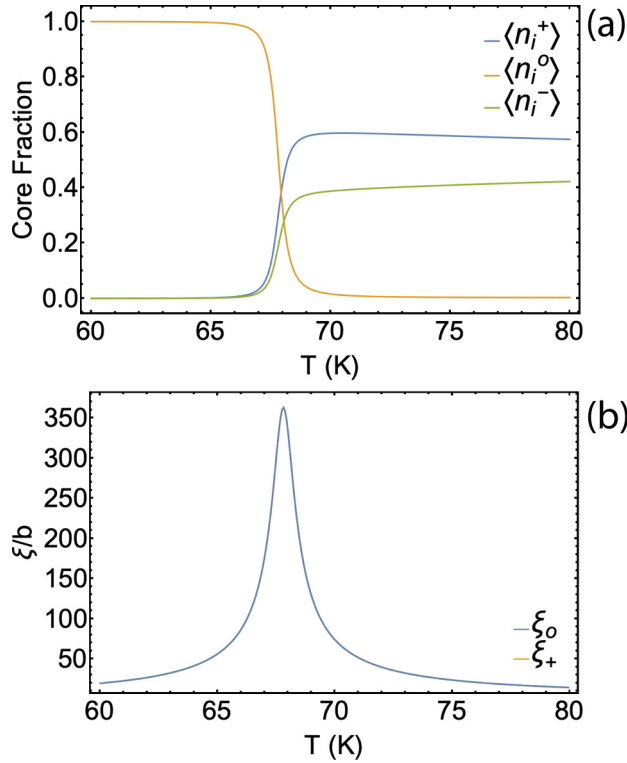


FIG. 11. (a) The composition of the dislocation for $\varepsilon_p = 0.001$ eV, $\Delta = -0.0005$ eV, $\delta = 0.0$ eV, $\kappa_{pp} = 0.01$ eV, and $\kappa_{op} = 0.04$ eV, for a dislocation containing $M = 10^4$ sites. (b) Correlation lengths for n^0 and n^+ using the same parameters.

the entropy driven switching transition and can broaden the temperatures over which the transition takes place. So in the case of core switching within the atomic scale simulations, care might be needed in exploring potential core switching behavior.

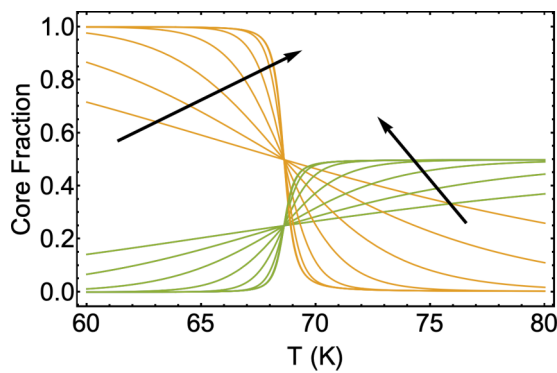


FIG. 12. The composition of the dislocation core as a function of temperature for varying periodic cell sizes. The parameters have been chosen the same as those used in Fig. 10, excepting that value of M , which is chosen to be 16, 32, 64, 128, 256, 512, and 1024. The gold curves are $\langle n_i^+ \rangle$. Here, the concentrations of “+” and “-” cores are equal, so the lines coincide, and only the lines for $\langle n_i^- \rangle$ are visible (green). The black arrows indicate the direction of increasing M for the sets of curves. The core composition at $M = 1024$ is essentially equal to that of the thermodynamic limit.

Finite size, however, can also be used to advantage. To see how this might be, consider that each dislocation segment chooses a plane upon which to spread. These planes can be designated by the angle they make with the basal plane. For example, a prism spread core will intersect the basal plane of the crystal at 90° . Similarly, a dislocation spread on the “+” pyramidal plane will make an angle of approximately 118.5° with the basal plane (depending upon the specific lattice constants), which corresponds to the an angle of 28.5° with the prism plane (corresponding to $\frac{c}{a} = 1.595$). Similarly, assuming the same $\frac{c}{a}$, the “-” pyramidal plane will make an angle of -28.5° with the prism plane. The instantaneous average angle, $\bar{\theta}$, that a dislocation’s spreading plane makes with the basal plane can be computed (in degrees)

$$\bar{\theta} = 90 + 28.5 \frac{1}{M} \sum_{i=0}^{M-1} \sigma_i. \quad (16)$$

The average angle during any time snapshot is simply proportional to the sum of the spins. The time average of $\bar{\theta}$ is proportional to $\langle \sigma_i \rangle$. This average angle, however, should display fluctuations in time. In the thermodynamic limit, the fluctuations from this average value are expected to go to zero. But for finite size systems, the fluctuations are observable, and they have a characteristic distribution that can be computed. Since molecular dynamics simulations are always finite sized, these fluctuations can be observed and analyzed (though this has not yet been done). So the angle distributions can be used to make contact between the simple model and molecular dynamics simulations. In order to make more progress, however, we need to compute the angle distributions, $P(\bar{\theta})$ within the simple model.

The distribution of the sum of spins can be derived from the partition function using the fact that the sum over the spins is always given by an integer. The probability that the sum of spins equals the integer N , then, is formally given by

$$P(N) = \frac{1}{Z} \sum_{\sigma_0=-1}^1 \cdots \sum_{\sigma_{M-1}=-1}^1 \exp[-\beta E_{\text{core}}(\{\sigma_i\})] \delta_{N, \sum_{i=0}^{M-1} \sigma_i}, \quad (17)$$

with $\delta_{n,m}$ the Kronecker delta function of the integers n and m . The evaluation of the sum can be carried out by introducing the integral representation of the Kronecker delta function:

$$\delta_{n,m} = \frac{1}{2\pi} \int_0^{2\pi} d\phi \exp[i\phi(n-m)]. \quad (18)$$

Substitution of Eq. (18) into Eq. (17) yields:

$$P(N) = \frac{1}{2\pi Z} \int_0^{2\pi} d\phi \exp[i\phi N] \sum_{\sigma_0=-1}^1 \cdots \sum_{\sigma_{M-1}=-1}^1 \exp[-\beta E_{\text{core}}(\{\sigma_i\})] \exp\left[-i\phi \sum_{i=0}^{M-1} \sigma_i\right]. \quad (19)$$

The constrained sum, then, effectively adds a term to the transfer matrix. Once this term is added, the summation is performed, and the remaining three integrals (one for each eigenvalue of the transfer matrix) are performed numerically to compute the probability distribution $P(N)$ and hence the

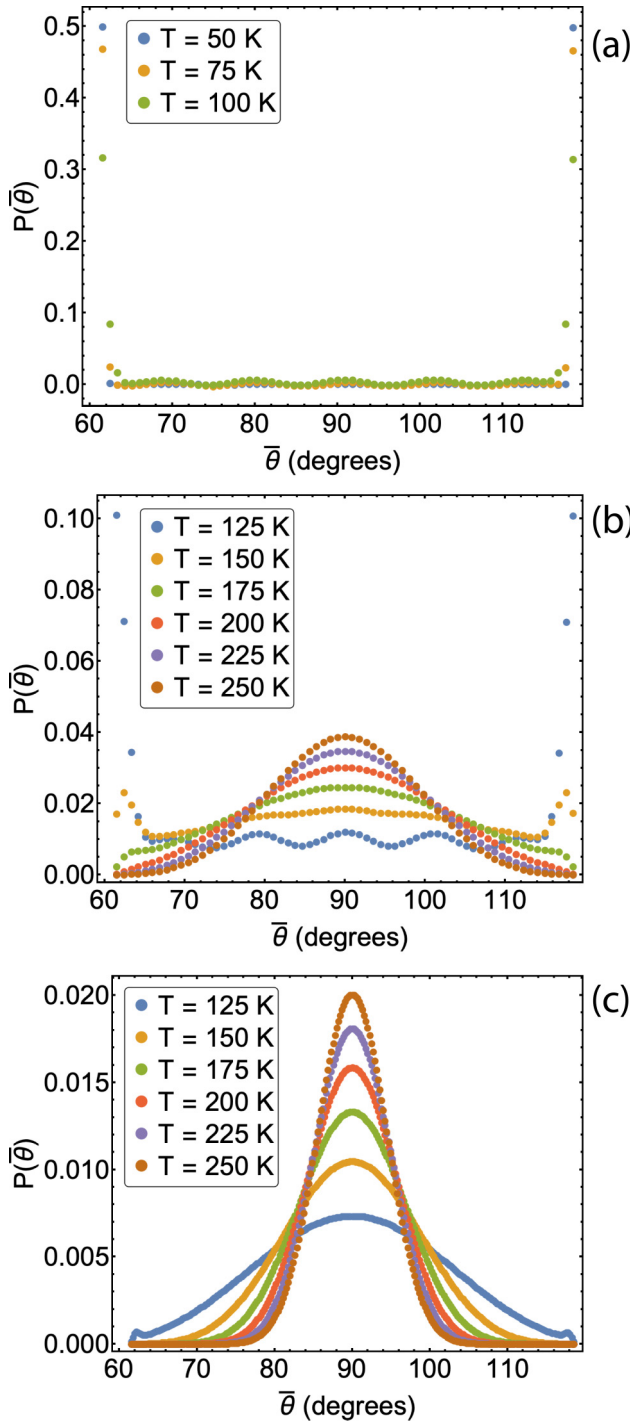


FIG. 13. Angle distributions for a dislocation with $\epsilon_p = -0.021$ eV, $\kappa_{op} = 0.01$ eV, $\kappa_{pp} = 0.04$ eV, $\Delta = \delta = 0.0$ eV, and $M = 32$ [panels (a) and (b)] and $M = 128$ [panel (c)] for different temperatures. The distributions are only defined for discrete values of $\bar{\theta}$.

probability distribution $P(\bar{\theta})$. Figure 13 displays the computed distribution of $\bar{\theta}$ for $\epsilon_p = -0.021$ eV, $\kappa_{op} = 0.01$ eV, $\kappa_{pp} = 0.04$ eV, $\Delta = \delta = 0.0$ eV, and $M = 32$ for different temperatures. Note that within this model the probability is defined only for certain discrete values of $\bar{\theta}$. Hence these plots are not approximations to a curve, but rather, the plots report

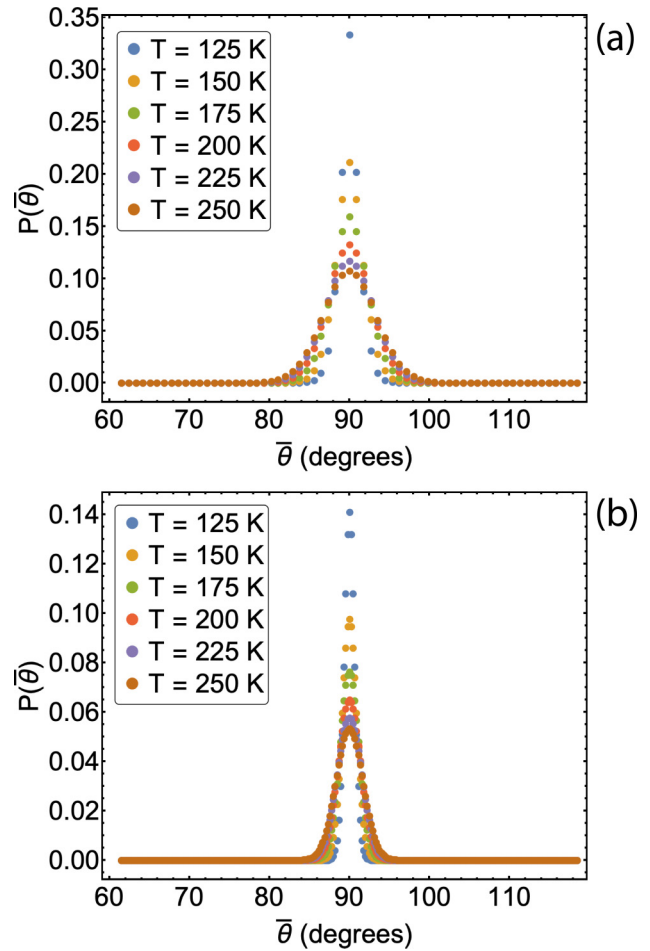


FIG. 14. Angle distributions for a dislocation with $\epsilon_p = 0.021$ eV, $\kappa_{op} = 0.01$ eV, $\kappa_{pp} = 0.04$ eV, $\Delta = \delta = 0.0$ eV for (a) $M = 32$ and (b) $M = 128$. The distributions are only defined for discrete values of $\bar{\theta}$.

a set of probabilities in graphical form. At low temperatures for the parameters chosen here, essentially no core segments are spread on the prism plane, even though the average value of $\theta = 90^\circ$. As the temperature warms, the prism segments become more common, and the initially bimodal distributions become unimodal. The cores, however, remain primarily spread on the pyramidal planes, but with equal probability, driving the distribution to be peaked about $\theta = 90^\circ$. Another interesting aspect of the low-temperature behavior is shown by the plot for $T = 50$ K. Here, the probability for the most extreme value of the angles is quite large in comparison to the remaining probabilities. Thus at low temperatures, the perfectly ordered state, for this system with $M = 32$, occurs with a finite probability (over 90% if one considers both possible pyramidal core spreadings). For $M = 128$, the distributions are more sharply peaked about $\theta = 90^\circ$. This is reasonable, as the larger the system one examines, the lower the variation in the mean of a parameter.

The behavior of the angle distribution when prism core segments are favored is shown in Fig. 14. Here, the distribution starts peaked at the completely prism ground state, and then grows broader with increasing temperature. Note, however,

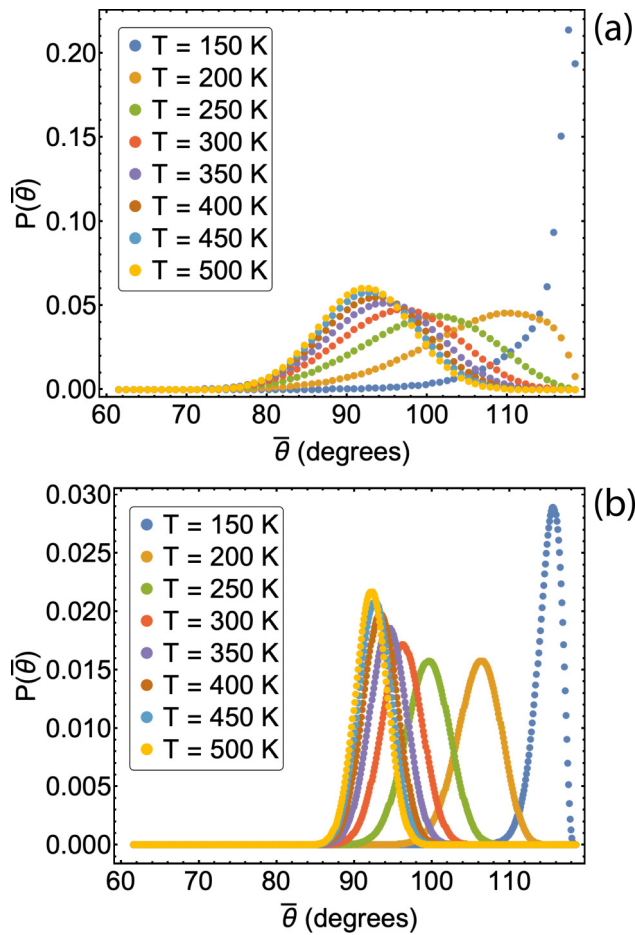


FIG. 15. Comparison of angle distributions for a dislocation with $\varepsilon_p = 0.021$ eV, $\kappa_{op} = 0.01$ eV, $\kappa_{pp} = 0.04$ eV, $\Delta = -0.01$ eV, $\delta = 0.0$ eV for (a) $M = 32$ and (b) $M = 256$, plotted for various temperatures. The distributions are only defined for discrete values of $\bar{\theta}$.

that the distribution for prism spread cores is narrower, at a given temperature, than that for pyramidal spread cores. Finally, the dependence of the distribution width on temperature is opposite for the two cases: pyramidal spread dislocations show a distribution with decreasing width as temperature increases, whereas the widths of the distributions for prism spread cores increase with temperature.

Of course, the $\bar{\theta}$ distributions depend on the size of the system. One obvious dependence is that an increase in system size increases the number of accessible values of N , because $-M \leq N \leq M$. This implies that the probability of encountering each individual angle is reduced, and this is reflected in the computed distributions. A second dependence has to do with the width of the probability distribution. As M increases, the width of the distribution $P(\bar{\theta})$ decreases (for a given temperature).

It is also interesting to explore the evolution of the angle distributions in the case that the symmetry is broken. Consider a dislocation described by $\varepsilon_p = -0.021$ eV, $\kappa_{op} = 0.01$ eV, $\kappa_{pp} = 0.04$ eV, $\delta = 0.0$ eV, $\Delta = -0.01$ eV. This distribution will favor the n^+ dislocation segments, and should lead to distribution peaked at an angle greater than 90° . In fact, symmetry breaking between the two pyramidal dislocation

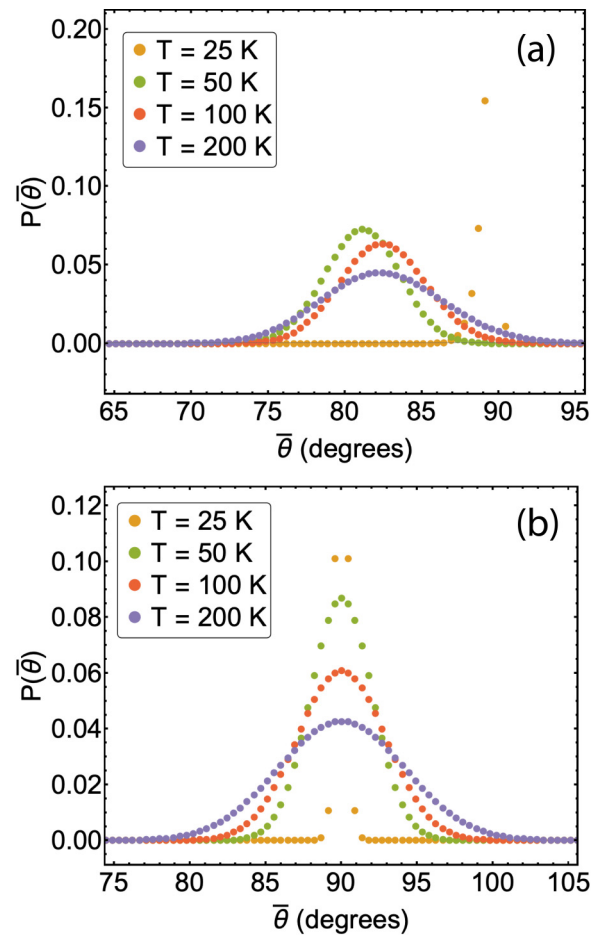


FIG. 16. The angle distributions in the case of parameters varying with temperature as shown in Fig. 8. For both panels, $M = 64$. (a) The plotted distributions in the broken symmetry case, with $\Delta = 0.007$ eV. (b) The distributions plotted in the case that $\Delta = 0.0$ eV. In both panels, the maximum for $T = 25$ K has been cropped from the plot.

cores is the only way to have an angle distribution peaked away from 90° , 61.5° , and 118.5° (given that $\frac{\varepsilon}{a}$ is chosen as above). A distribution with a peak angle differing from these values is one necessarily corresponding to the broken symmetry case. Figure 15 displays the angle distributions for these parameters. In this circumstance, the distributions are skewed as expected. At very low temperatures, the skewing is extreme. As the dislocation is warmed, however, the average angle moves away from the limiting value and more towards 90° .

Finally, it is interesting to consider what will happen to the angle distributions near the switching transition. Figure 16 displays the distributions expected for the same parameters as used in Fig. 8, excepting that $M = 64$ and in panel (b) the symmetric case ($\Delta = 0.0$ eV) is considered. Note that the distribution width increases monotonically with temperature over the range of temperatures plotted.

Figure 17 displays an example of the angle distributions computed through the entropy driven switching transition shown in Fig. 9, for a dislocation with $M = 256$. Below the switching transition, the finite system is completely in

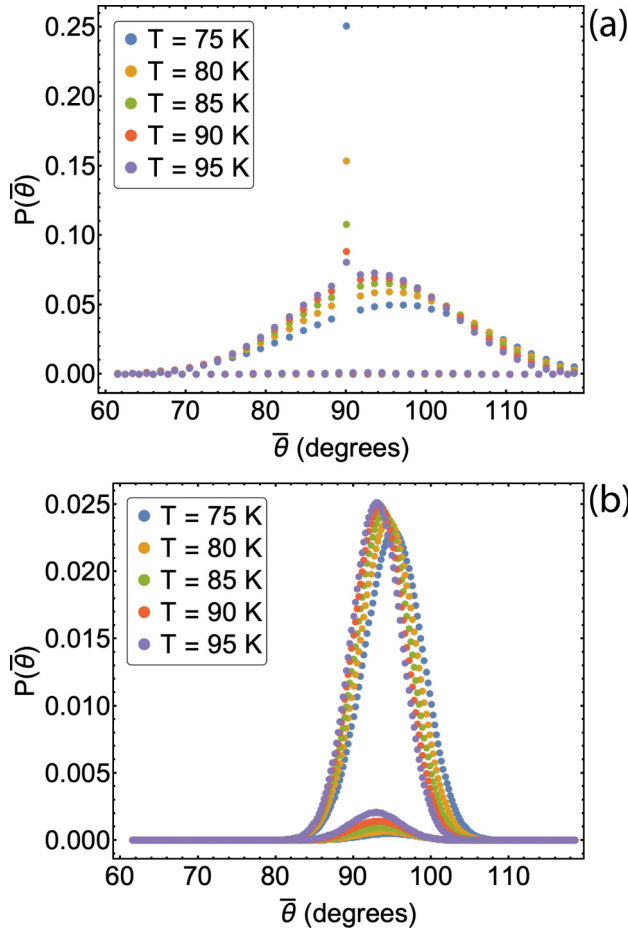


FIG. 17. Comparison of angle distributions for a dislocation with $\varepsilon_p = 0.001$ eV, $\kappa_{op} = 0.04$ eV, $\kappa_{pp} = 0.01$ eV, $\Delta = -0.0005$ eV, $\delta = 0.0$ eV and (a) $M = 32$, (b) $M = 256$ shown at various temperatures. The distributions are only defined for discrete values of $\bar{\theta}$.

the prism spread state, and, essentially, $P(90^\circ) = 1$. As the temperature is increased, there is still a significant probability to find the dislocation core prism dissociated, but the probability to find the favored pyramidal spreading is increased. Eventually, the probability to find the prism spread core drops to, essentially, zero, and the distribution is dominated by the pyramidal spread core states. These states, however, are near symmetric, as the symmetry breaking is quite small for this set of parameters.

It is also apparent that once the pyramidal segments become the dominant, the distribution has the property that the probability of every other angle is markedly reduced relative to its neighbors. This is because a flip from one pyramidal core to the next, changes the average of $\langle \sigma_i \rangle$ by an increment of $\frac{2}{M}$. The only way to change the average spin by an increment $\frac{1}{M}$ is to introduce a prism core state, which has a very low probability of appearing immediately above the transition temperature. In this plot, sums of σ_i that are even are more common because M is chosen to be even. If M is chosen to be odd, then the most common sums of σ_i would be odd as well.

In Ref. [28], angle distributions are computed. Those distributions, however, differ from those considered here in that they measure the angle at each segment, for many differ-

ent snapshots in time, and lump all the segment data from different times together in order to generate a time average of the angle distribution. In the thermodynamic model, since there are only three possible orientations, these distributions would appear as three simple spikes at the fixed angles. In contrast, $P(\bar{\theta})$ measures the distribution of average angle over an entire dislocation. This data is in principle accessible to MD simulations, but has not yet been analyzed.

Nevertheless, an interesting observation can be made. In the simple model, the distribution for $P(\bar{\theta})$ is symmetric about $\bar{\theta} = 90^\circ$ as long as $\Delta = \delta = 0.0$ eV. The symmetry breaking requires that the stress favor one configuration over another. MD dynamics simulations of dislocations within periodic supercells appear to show the symmetry breaking, which suggests that the stresses from the periodic environment might be breaking the symmetry between the two pyramidal core spreadings. However, this conclusion might be in error. The exact solution for the thermodynamic model does not tell one anything about the dynamics. According to the ergodic hypothesis, the time average of the phenomenon should be equal to the thermodynamic expectation. However, the time scales over which one must average is unknown. Given this, it is possible that the MD simulations considered thus far have not yet been run for times long enough for the results to be ergodic.

IV. CONCLUSIONS

In this paper, a simple model aimed at computing the configurational contributions to the free energy of a dislocation arising from core spreading polymorphism is introduced and studied. The thermodynamic properties of the model are computed exactly, and in most cases analytically. It is shown that the configurational contributions to the free energy at room temperature can be comparable to the total energy difference computed at zero temperature. It is also demonstrated that, at temperature, it is likely that an individual dislocation is composed of segments that are a mix of all three spreadings, or, perhaps, a mix of both types of pyramidal spreading, depending on the specific parameters describing the dislocation.

The possibility for dislocation core switching is explored. The simple model allows for transitions in the core structure driven by an increase in temperature. These can come about at fixed model parameters, or perhaps, through the temperature dependence of the parameters themselves. The former case is considered in some detail, and it is noted that for certain choices of the parameters, the pyramidal cores can have more entropy accessible at lower temperatures. This can lead to a dislocation core switching transition in which the predominant core spreading morphology changes rather abruptly over a small temperature range. It is noted that such transitions will strongly influence dislocation dynamics, and hence may complicate modeling.

Correlation lengths are examined. It is found that for most parameters choices and temperatures of interest, correlation lengths are quite small, as are domain sizes. The implication is that small simulations, the size of those accessible to atomic scale computation, are in many cases sufficient. However,

under certain circumstances, the correlation lengths can grow to $300b$ or more. One example is during the entropy driven core switching transition. Another instance is for very low temperatures, where the $+$ pyramidal plane symmetry is not broken.

Given the size limitations for atomic scale simulations, it is of some interest to identify parameters that can be assessed using smaller scale simulations. One such parameter is the angle the dislocation core spreading plane makes with the basal plane. The simple model was used to calculate the distribution of these angles, and the dependence of these distributions on the parameters of the model are explored. It is noted that asymmetry in the pyramidal core spreading energies was the

only way to obtain a distribution not centered on the prism plane in the ergodic limit.

ACKNOWLEDGMENTS

The authors gratefully acknowledge funding from the US Office of Naval Research under Grants No. N00014-16-S-BA10 (D.C.C. and I.W.) and Grants No. N00014-16-1-2304 and No. N00014-19-1-2376 (M.P. and M.A.). This research used the Savio computational cluster resource provided by the Berkeley Research Computing program at the University of California, Berkeley (supported by the UC Berkeley Chancellor, Vice Chancellor for Research, and Chief Information Officer).

-
- [1] J. Hirth and J. Lothe, *Theory of Dislocations* (Krieger Publishing Company, Malabar, FL, 1982).
- [2] R. Peierls, *Proc. Phys. Soc.* **52**, 34 (1940).
- [3] F. R. N. Nabarro, *Proc. Phys. Soc.* **59**, 256 (1947).
- [4] J. Bennetto, R. W. Nunes, and D. Vanderbilt, *Phys. Rev. Lett.* **79**, 245 (1997).
- [5] X. Blase, K. Lin, A. Canning, S. G. Louie, and D. C. Chrzan, *Phys. Rev. Lett.* **84**, 5780 (2000).
- [6] N. Lehto and S. Öberg, *Phys. Rev. Lett.* **80**, 5568 (1998).
- [7] S. Beckman and D. C. Chrzan, *Phys. B: Condens. Matter* **340-342**, 990 (2003).
- [8] A. Valladares and A. P. Sutton, *J. Phys.: Condens. Matter* **17**, 7547 (2005).
- [9] L. Pizzagalli, P. Beauchamp, and H. Jónsson, *Philos. Mag.* **88**, 91 (2008).
- [10] R. Chang and L. J. Graham, *Phys. Status Solidi B* **18**, 99 (1966).
- [11] R. Chang, *Philos. Mag.* **16**, 1021 (1967).
- [12] M. S. Duesbery, *Philos. Mag.* **19**, 501 (1969).
- [13] V. Vitek, R. C. Perrin, and D. K. Bowen, *Philos. Mag.* **21**, 1049 (1970).
- [14] V. Vitek, *Cryst. Lattice Defects* **5**, 1 (1974).
- [15] L. Romaner, C. Ambrosch-Draxl, and R. Pippan, *Phys. Rev. Lett.* **104**, 195503 (2010).
- [16] D. J. H. Cockayne and V. Vitek, *Phys. Status Solidi B* **65**, 751 (1974).
- [17] Y. Minonishi, S. Ishioka, M. Koiwa, S. Morozumi, and M. Yamaguchi, *Philos. Mag. A* **43**, 1017 (1981).
- [18] M. H. Liang and D. J. Bacon, *Philos. Mag. A* **53**, 181 (1986).
- [19] E. Clouet, *Phys. Rev. B* **86**, 144104 (2012).
- [20] E. Clouet, D. Caillard, N. Chaari, F. Onimus, and D. Rodney, *Nat. Mater.* **14**, 931 (2015).
- [21] C. R. Miranda, R. W. Nunes, and A. Antonelli, *Phys. Rev. B* **67**, 235201 (2003).
- [22] G. Lu, N. Kioussis, V. V. Bulatov, and E. Kaxiras, *Phys. Rev. B* **62**, 3099 (2000).
- [23] P.-A. Geslin and D. Rodney, *Phys. Rev. B* **98**, 174115 (2018).
- [24] Y. Jiang, R. Wang, and S. Wang, *Philos. Mag.* **96**, 2829 (2016).
- [25] S. Farenc, D. Caillard, and A. Couret, *Acta Metall. Mater.* **43**, 3669 (1995).
- [26] P. Kwasniak and H. Garbacz, *Acta Mater.* **141**, 405 (2017).
- [27] M. Poschmann, M. Asta, and D. C. Chrzan, *Modell. Simul. Mater. Sci. Eng.* **26**, 014003 (2018).
- [28] M. Poschmann, I. S. Winter, M. Asta, and D. C. Chrzan, *Phys. Rev. Materials* **6**, 013603 (2022).
- [29] E. Ising, *Z. Phys.* **31**, 253 (1925).
- [30] R. G. Hennig, T. J. Lenosky, D. R. Trinkle, S. P. Rudin, and J. W. Wilkins, *Phys. Rev. B* **78**, 054121 (2008).
- [31] M. Poschmann, M. Asta, and D. C. Chrzan, *Comput. Mater. Sci.* **161**, 261 (2019).